Fuel 128 (2014) 113–119

Contents lists available at ScienceDirect

Fuel

journal homepage: www.elsevier.com/locate/fuel

Catalytic conversion of glycerol to oxygenated fuel additive in a continuous flow reactor: Process optimization

Malaya R. Nanda [a], Zhongshun Yuan [a], Wensheng Qin [b], Hassan S. Ghaziaskar [c], Marc-Andre Poirier [d], Chunbao (Charles) Xu [a,*]

[a] *Department of Chemical & Biochemical Eng., Western University, London, ON N6A 5B9, Canada*
[b] *Department of Biology, Lakehead University, ON P7B 5E1, Canada*
[c] *Department of Chemistry, Isfahan University of Technology, Isfahan 84156-83111, Iran*
[d] *Imperial Oil Limited, Supply Support and Environmental Group, ON N7T 8C8, Canada*

HIGHLIGHTS

- A continuous flow process for synthesis of solketal from glycerol was optimized.
- A maximum yield of 94 ± 2% was obtained at optimum conditions.
- Presence of impurities (salt and water) demonstrated an adverse effect on the yield.
- The catalyst after 24 h on-stream use proved to be regenerable.

GRAPHICAL ABSTRACT

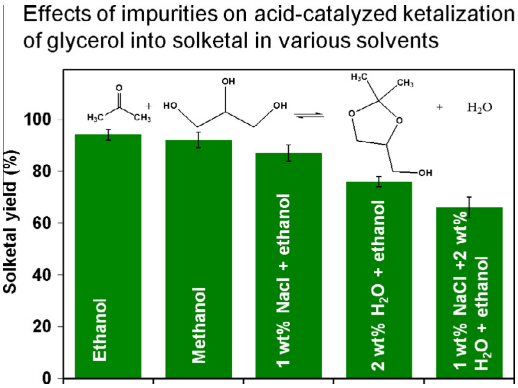

ARTICLE INFO

Article history:
Received 19 December 2013
Received in revised form 23 February 2014
Accepted 26 February 2014
Available online 12 March 2014

Keywords:
Continuous flow reactor
Catalyst
Glycerol
Ketalization
Solketal

ABSTRACT

A continuous-flow process using ethanol solvent and heterogeneous catalyst amberlyst-36 was developed for conversion of glycerol to solketal, an oxygenated fuel additive, and the process was optimized in this study using response surface methodology. A model was proposed based on Box-Behnken design. At optimum conditions (temperature of 25 °C, acetone-to-glycerol molar ratio of 4 and weight hour space velocity of 2 h^{-1}) the maximum yield was obtained at 94 ± 2%. The presence of impurities such as water and salt in glycerol significantly reduced the yield at the optimum conditions. The catalyst could be regenerated and reused for 24 h with an insignificant sign of deactivation. The use of methanol as solvent at the optimal conditions proved to be potential in making the system more economical. The economic analysis for the process revealed the potential of converting glycerol into solketal – an alternative to methyl tert-butyl ether as fuel additive.

© 2014 Elsevier Ltd. All rights reserved.

1. Introduction

The world biodiesel production has been boosted in recent years owing to an increasing demand of renewable and sustainable energy. Glycerol is produced as a byproduct in the process of biodiesel production. The amount of glycerol generated is approximately 10 wt% of the biodiesel produced in a conventional biodiesel process [1,2]. Hence a huge amount of glycerol is expected on the market in near future. Due to saturation of the glycerol market, the extra glycerol is now being considered as a

---

* Corresponding author. Tel.: +1 (519)661 2111x86414; fax: +1 (519)661 4016.
E-mail address: cxu6@uwo.ca (C. (Charles) Xu).

http://dx.doi.org/10.1016/j.fuel.2014.02.068
0016-2361/© 2014 Elsevier Ltd. All rights reserved.

waste by many biodiesel producers and going to affect the sustainability of the biodiesel industry [3].

In this context, it is important to find some value added applications of glycerol. Upgrading glycerol into different valuable chemicals has been reported [4–7]. Acetalization of glycerol is one of the methods considered to be promising and economically viable for the utilization of glycerol [8]. In this process, glycerol reacts with an aldehyde or a ketone to form an acetal or a ketal, respectively, in the presence of an acid catalyst [9].

Solketal (2,2-dimethyl 1,3-dioxalane-4-methanol) is a ketal formed by the acid catalyzed reaction between glycerol and acetone [10]. Roldan et al. reported the synthesis of solketal from glycerol using a zeolite membrane batch rector, where a high amount of acetone was used (an equivalent ratio of 20) with 82% yield of solketal [11]. In another work, Vicente et al. [5] reported 89.5% yield of solketal in a two step batch process with an acetone equivalent ratio of 6. Important applications of solketal include being used as an additive to improve transportation fuel properties, as a plasticizer in polymer industry and a solvent in pharmaceutical industry [4,12,13].

Response surface methodology (RSM) is a technique generally used for modeling and optimization of the experimental observations in physical and chemical processes. The key aim of using RSM is to optimize the surface response and to determine the relationship between the input variables and the response data [14].

The operational conditions for an optimum yield of solketal have been investigated in batch reactors [7,5,13]; however hardly any attempt has been made for the process optimization in a continuous-flow reactor.

From our preliminary experiments for the catalytic conversion of glycerol to oxygenated fuel additive in a continuous flow reactor, amberlyst-36 was found to be the best catalyst among others based on the yield and the catalyst's stability on stream [16]. Process parameters including temperature (in the range 25–65 °C), acetone-to-glycerol equivalent ratio (in the range of 2–6 mol/mol) and weight hourly space velocity (WHSV) (range of 2–4 h^{-1}) are considered to have significant effect on the product yield.

The present study mainly dealt with the optimization of the catalytic conversion of glycerol to solketal as an oxygenated fuel additive in a continuous flow reaction process. In this study, the optimization method was used to obtain a maximum yield in the shortest reaction time and at the lowest cost. RSM technique was applied in the process optimization study and a quadratic model was proposed based on Box–Behnken design (BBD) including the interactions of the process variables.

2. Experimental

2.1. Materials

Glycerol, methanol, and acetone (both >99 wt% purity) were procured from Sigma–Aldrich and used as received, and commercial grade ethanol was supplied from Commercial Alcohols Inc., Solketal [(S−) (+) – 1,2-Isopropylideneglycerol, 99 wt%] was also obtained from Sigma–Aldrich as a calibration standard for GC analysis. The solid acid catalyst: Amberlyst – 36 (Wet) was obtained from Rohm and Hass Co. (USA) and its key characteristics are listed in Table 1. Hereafter the catalyst will be simply referred to as amberlyst.

2.2. Experimental procedure

The experiments were carried out in a continuous-flow reactor system whose details were given in our recently published work [16]. The ketalization reaction was carried out in a 316-stainless steel tubular reactor (ID: 7.7 mm, OD = 9.5 mm and length: 60 cm) placed in a tube furnace (model# 21135, Thermolyne). The reactor was loaded with a given amount of catalyst (typically 2 g) with Pyrex wool as bed supporter. The feed was a mixture of acetone (A), glycerol (G) and ethanol (E) solvent at a specific molar ratio of A:G:E = X:1:1 where X is the acetone-to-glycerol equivalent ratio (varying from 2 to 6 mol/mol in this study). In a typical run, the feed containing a calculated amount of acetone and glycerol with ethanol as solvent were well mixed and pumped into the reactor with a HPLC pump (Lab Alliance series II) at a predetermined flow rate, depending on the target weight hourly space velocity (WHSV). The WHSV is defined as:

$$\mathrm{WHSV}\ (h^{-1}) = \frac{\text{Flow of glycerol per hour (g/h)}}{\text{Weight of catalyst (g)}} \tag{1}$$

The pressure of the reactor was controlled by a back pressure regulator and was kept constant throughout the experiment (500 psi). The product stream from the reactor was collected in every 20 min and was subject to further analysis for determination of glycerol conversion and solketal yield.

2.3. Product analysis

The main components in the product mixture were first qualitatively analyzed on a gas chromatograph, equipped with a mass selective detector [Varian 1200 Quadrupole GC/MS (EI), Varian CP-3800 GC equipped with VF-5 MS column (5% phenyl/95% dimethyl-polysiloxane, 30 m × 0.25 mm × 0.25 μm)], using helium as the carrier gas at a flow rate of $5 \times 10^{-7}\ m^3/s$. The oven temperature was maintained at 120 °C for 2 min and then increased to 200 °C at a ramp rate of 40 °C/min. Injector and detector block temperature were maintained at 300 °C. The components were identified using the NIST 98 MS library with the 2002 update. The concentrations of the components (mainly glycerol and solketal) were then quantified using a GC-FID (Shimadzu-2010) under the similar conditions as used for the GC–MS measurement.

The solketal yield and glycerol conversion were calculated using the following equations:

$$\text{Yield (mol\%)} = \frac{\text{Moles of solketal formed}}{\text{Initial moles of glycerol fed into the reactor}} \times 100\% \tag{2}$$

$$\text{Conversion (mol\%)} = \frac{\text{Reduction in moles of glycerol in the reaction}}{\text{Initial moles of glycerol fed into the reactor}} \times 100\% \tag{3}$$

2.4. Experimental design

Box–Behnken design (BBD) was applied in the optimization of the process. BBD is a class of rotatable second order design based on three level incomplete factorial designs [17]. The required number of experimental runs (N) for the development of BBD can be calculated from the following correlation [18]:

$$N = 2x(x-1) + C_0 \tag{4}$$

where x is the number of factors and C_0 is the number of central points in the design. In this study, temperature (25–65 °C), acetone equivalent ratio (2)–(6) and WHSV (2–4 h^{-1}) were three factors chosen for optimization and the yield of solketal is the only response in the ketalization study. Thus, from Eq. (4), a set of 17 runs (including 5 central points) were carried out. The different coded levels, −1 (low), 0 (central) and +1 (high) of the factors are given in Table 2. For statistical calculations, the relation between the coded values and real values were described as follows [19]:

Table 1
Catalyst characterization.

Catalyst	BET surface[a] (m^2/g)	Pore volume[a] (cc/g)	Pore size[a] (nm)	Acidity[b] (eq/g)
Amberlyst (Fresh)	35 (32)	0.28 (0.32)	16.8 (18.2)	5.5 (4.6)
Regenerated catalyst[c]	33 (37)	0.29 (0.33)	17.3 (18.5)	5.4 (4.4)

[a] Determined by N_2 isothermal adsorption.
[b] Determined by NH_3-TPD.
[c] Regenerated by 0.5 M dilute H_2SO_4 acid washing; Values in parenthesis are measured from the catalyst after 24 h on-stream of reaction.

$$X_i = \frac{x_i - \frac{(x_h + x_l)}{2}}{\frac{x_h - x_l}{2}} \tag{5}$$

where X_i is the dimensionless coded value (−1, 0, +1) of the *i*th independent variable, x_i is the un-coded (real) value of variable, x_h and x_l are the real value of x_i at its high and low level, respectively. The independent variables studied are temperature, acetone equivalent ratio and WHSV for X_1, X_2, and X_3 respectively. The relationship and interrelationships of the variables were determined by fitting the second order polynomial equation to data obtained and is given as:

$$Y = b_0 + b_1X_1 + b_2X_2 + b_3X_3 + b_{11}X_1^2 + b_{22}X_2^2 + b_{33}X_3^2 + b_{12}X_1X_2 + b_{13}X_1X_3 + b_{23}X_2X_3 + e \tag{6}$$

where Y is the predicted value, b_0 is the constant term, b_1, b_2 and b_3 are linear coefficients, b_{11},b_{22} and b_{33} are the quadratic coefficients, b_{12}, b_{13} and b_{23} are the cross product coefficients and *e* is the experimental error term. The BBD matrix is given in Table 3. Minitab software package was used for determining the regression coefficients of the model. Analysis of the variance (ANOVA) with Fisher's *F*-test was used to determine the statistical significance of the model coefficients. The fitted polynomial was expressed in three dimensional surface plot and contour plots to explain the relationship between the response and the levels of each parameter used in this study.

3. Results and discussion

3.1. Model fitting and statistical analysis

The measured response data for different coded combinations are given in above Table 3. The obtained results are the average values of three separate measurements which are rounded up to the nearest whole number with a relative standard deviation of 3.6% at 95% confidence level. A modified second order polynomial model, by eliminating the insignificant model terms, was used to fit the experimental data to obtain a regression equation using the coded factors as shown below:

$$Y = 83.42 - 5.63X_1 + 8.75X_2 - 6.63X_3 - 4.20X_2^2 - 2.95X_3^2 \tag{7}$$

The adequacy of the proposed model was verified by using the ANOVA technique. The ANOVA results are presented in Table 4. The *p*-value was used to check the significance of each coefficient. The smaller is the *p*-value, the more is the significance of the corresponding coefficient [20,21]. In this work, the *p*-value of the regression model is smaller than 0.000000, which suggested that the corresponding coefficient is significant and the model is suitable to be used in this experiment.

Table 2
Actual and corresponding coded values of each parameter.

Variables	Symbol	Levels		
		−1	0	1
Temperature (°C)	x_1	25	45	65
Acetone equivalent ratio	x_2	2	4	6
WHSV (h^{-1})	x_3	2	3	4

Table 3
Experimental design matrix and measured response values.

Run order	X_1	X_2	X_3	Response (yield %)
1	−1	0	1	78
2	0	0	0	83
3	−1	−1	0	75
4	0	0	0	85
5	−1	1	0	95
6	−1	0	−1	94
7	1	−1	0	65
8	0	0	0	82
9	0	1	−1	89
10	1	0	−1	83
11	0	−1	−1	74
12	1	0	1	67
13	0	0	0	83
14	1	1	0	82
15	0	1	1	80
16	0	0	0	84
17	0	−1	1	62

The lack-of fit measured the failure of the model to represent the data points which are not included in the regression. The *F*-value of 2.391 and *p*-value of 0.208731 represent that the lack-of-fit is insignificant relative to the pure error [22].

Adequate precision compares the predicted values at the design points to the average prediction error. In this study, the adequate precision was calculated and found to be greater than 4. This high adequate precision value indicates that the model is competent to navigate through the design space and is able to predict the response accurately.

The regression coefficients and the corresponding *p*-values for all the model terms are given in Table 4. From *p*-values of each model term, it may be concluded that all the independent variables (X_1, X_2, and X_3) and the quadratic terms (X_2^2 and X_3^2) significantly affect the yield of solketal.

The coefficient of determination, R^2, indicates the overall predictability of the model. It often shows how the model approximates the experimental data and can be defined as [23]:

$$R^2 = \frac{SS_{Model}}{SS_{Total}} = 1 - \frac{SS_{Error}}{SS_{Total}} \tag{8}$$

where SS_{Model}, SS_{Error}, and SS_{Total} are sum square model, sum square error, and sum square total, respectively. The R^2 value for the model was found to be 0.9802. It may be assumed that 98.02% of the total variations in the response could be explained by the model [24,25]. However, this large value of R^2 does not necessarily indicate that the model is a suitable one. The adjusted R^2 is defined to correct the R^2 value. In this experiment, the obtained adjusted R^2 value was found to be 0.9712. The very close value of adjusted R^2 to R^2 suggests a high significance of the model. The variation of the model can also be explained by calculating the coefficient of variation (CV). In this model, the calculated low value of coefficient of variation

Table 4
ANOVA analysis for the reduced quadratic model of yield.

Source	Sum of squares	Degree of freedom	Mean squares	*F* value	*p*-value
Model	1333.98	5	266.796	108.854	0.000000
X_1	253.13	1	253.125	103.276	0.000001
X_2	612.50	1	612.500	249.902	0.000000
X_3	351.12	1	351.125	143.260	0.000000
X_2^2	74.39	1	74.387	30.350	0.000184
X_3^2	36.68	1	36.678	14.965	0.002615
Residual	26.96	11	2.451		
Lack of fit	21.76	7	3.109	2.391	0.208731
Pure error	5.20	4	1.300		
Total	1360.94	16			

was 1.43%, suggesting a very high degree of accuracy and confidence of tests [15].

The relationship between the experimental and model predicted values of solketal yield is given in Fig. 1. The points around the diagonal line imply that the deviation between the experimental and the predicted values is less. Hence, it can be concluded that the values calculated from the model equation are very close to those obtained from the experiments, again suggesting the high accuracy of the proposed model. Moreover, the deviations can be explained by calculating the average absolute deviation (AAD) given by the following equation [18]:

$$\text{Average Absolute Deviation (AAD)} = \left[\frac{\sum_{i=1}^{n}\left(\frac{|y_{i,exp}-y_{i,pre}|}{y_i\,\text{exp}}\right)}{n}\times 100\right] \tag{9}$$

where $y_{i,pre}$ and $y_{i,exp}$ are the predicted and the experimental results, respectively with n as the experimental runs. The value of AAD was found to be 1.16%. The values of both R^2 and AAD confirmed that the given model defines the true behavior of the system.

The distribution of the data was determined by the probability plot displayed in Fig. 2, which indicates a well normal distribution and the independence of the residuals [20].

3.2. Response surface analysis

The single effect of each parameter on the yield of solketal is shown in Fig. 3, which is generally termed as the matrix plot. It was plotted by considering the mean value of the yield at each coded point. From the plot, it is clear that the solketal yield was increased by the decrease in temperature (X_1) and weight hour space velocity (X_3) and increase in the acetone equivalent ratio (X_2). This was expected as the reaction is exothermic, and a higher WHSV means a shorter contact time of glycerol with the catalyst, which reduced the glycerol conversion. The increase in the solketal yield with acetone equivalent is attributed to the presence of large amount of acetone. This excess reactant shifts the reaction equilibrium towards the products. Furthermore, the excess acetone acts as an entrainer and removes water from the reaction media which helps to drive the equilibrium towards the production of solketal [5]. These results are supported by the data presented in previous Table 4, which indicates that the acetone equivalent ratio and the WHSV are the most effective individual factors on the yield of

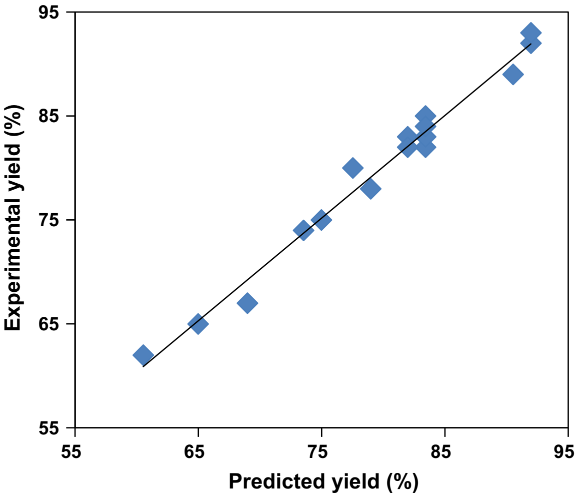

Fig. 1. The experimental results versus the model predicted results.

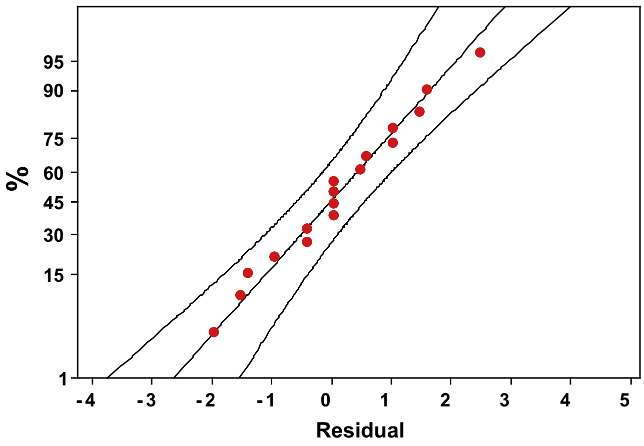

Fig. 2. The normal probability plot of the residuals.

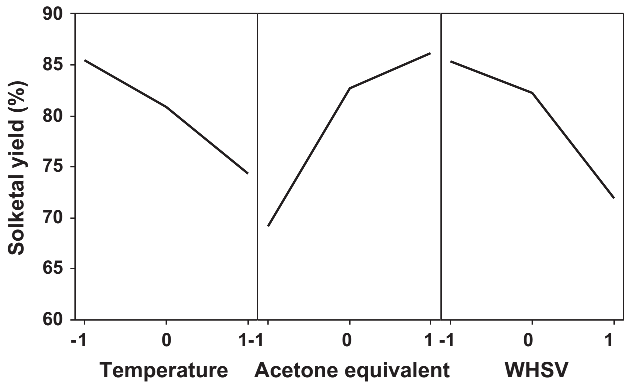

Fig. 3. Matrix plot of X_1 (temperature), X_2 (acetone equivalent ratio) and X_3 (WHSV).

solketal (acetone equivalent ratio: *F*-value – 249.902 and *p*-value – 0.000000, WHSV: *F*-value – 143.260 and *p*-value – 0.000000).

The response surface and contour plots of the model are given in Figs. 4(a–c) and 5(a–c). Three dimensional response surface plots and two-dimensional contour plots are very useful to analyze the interaction effects of different factors on the response. The response surface plot mainly explains the sensitiveness of the response towards the change of variables where as the contour plot describes the significant coefficient between the variables [26,27]. These plots explain the effect of two factors on the response at a time, keeping the third factor constant at level zero.

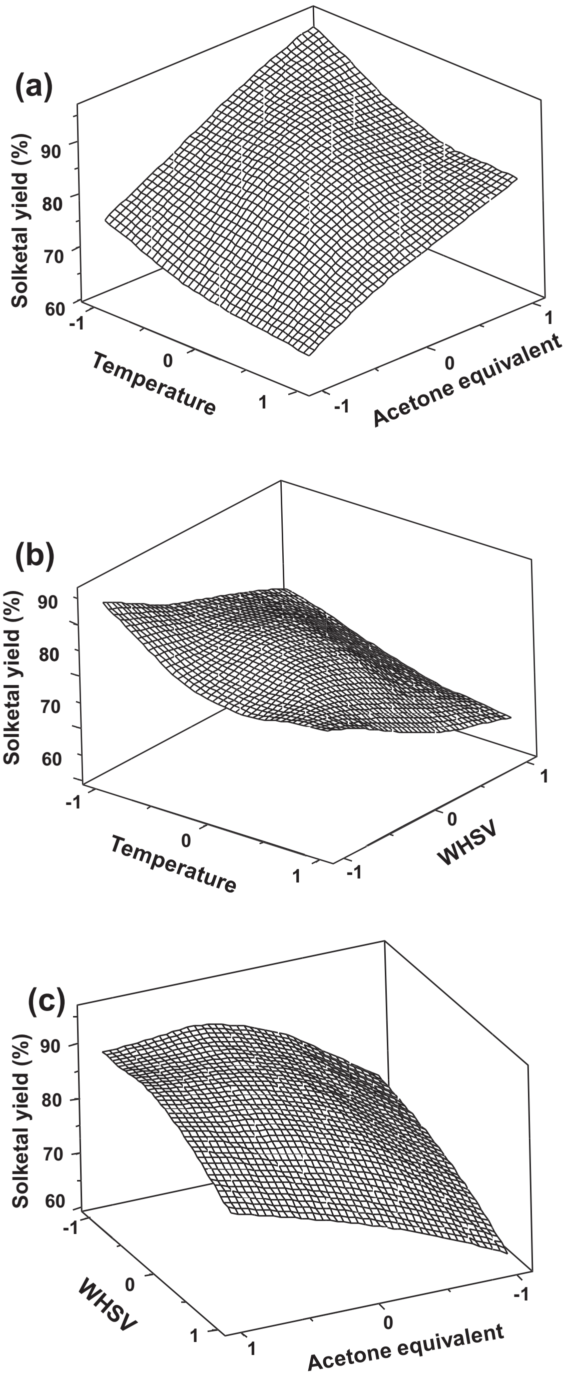

Fig. 4. Surface plots for effects of temperature and acetone equivalent ratio on solketal yield (a), effect of temperature and WHSV on solketal yield (b) and effect of acetone equivalent ratio and WHSV on solketal yield (c).

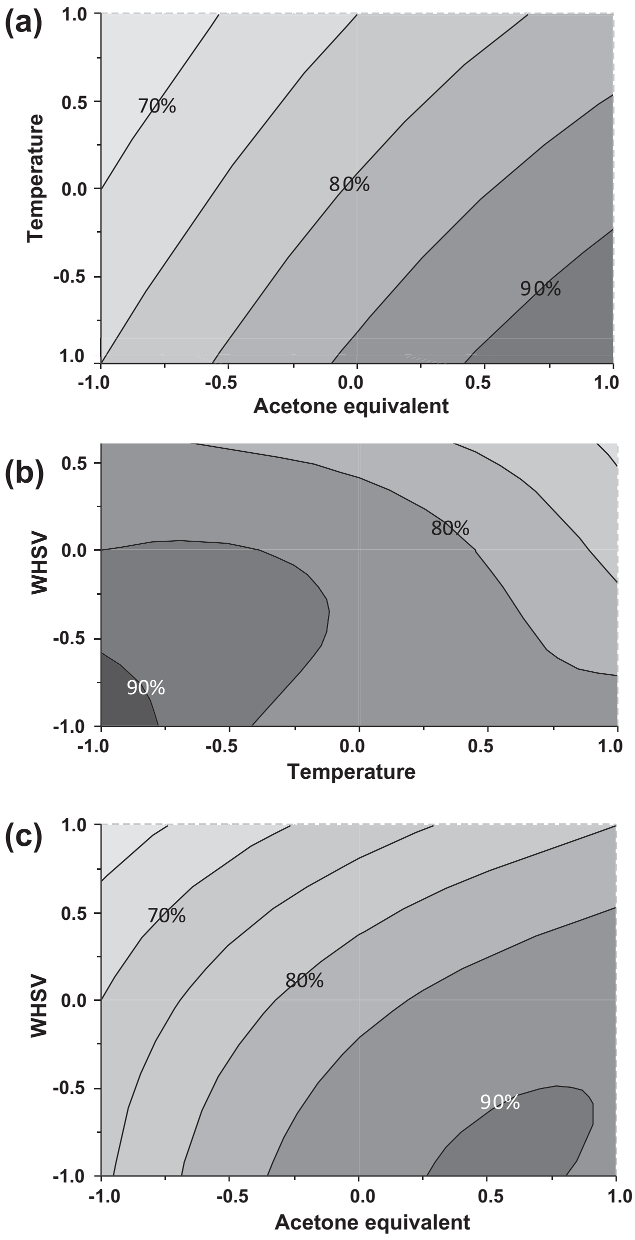

Fig. 5. Contour plots for effects of temperature and acetone equivalent ratio on solketal yield (a), effect of temperature and WHSV on solketal yield (b) and effect of acetone equivalent ratio and WHSV on solketal yield (c).

The dependence of the solketal yield on the mutual interaction between temperature and acetone equivalent ratio can be best interpreted from the response surface and the contour plot given in Figs. 4a and 5a, which indicated that the solketal yield is inversely related to the temperature and directly related to the acetone equivalent ratio. As explained earlier, a high acetone equivalent ratio drives the reaction towards the product side to result in a higher yield. In the contour plot, no interaction effect between the temperature and acetone equivalent was observed. The maximum yield was obtained at a temperature around −1 (coded value) and the acetone equivalent ratio of around 1 (coded value).

Figs. 4b and 5b represented the effects of temperature and WHSV on the yield of solketal. It can be seen that both temperature and WHSV have similar effects on the yield, i.e., inversely proportional to the yield. The reaction temperature has a little effect on the yield of solketal when the WHSV is kept in between 0 and 1 (coded values). However a remarkable enhancement in the solketal yield (from 85% to 95%) was observed at a lower temp (coded value: 0 to −1) and at a lower WHSV (coded value 0 to −1). This indicates that a lower temperature and lower WHSV are the favorable conditions to achieve a higher yield (close to 100%) of solketal.

The effects of acetone equivalent ratio and WHSV on the solketal yield could be seen in Figs. 4c and 5c. A maximum yield (~95%) was observed at a lower WHSV (coded value −1) and a higher acetone equivalent ratio (coded value between 0 and 1).

3.3. Optimization of reaction parameters

In this study, the main objective was to find the conditions where maximum solketal yield can be obtained. The optimal values of the selected parameters obtained from the regression model and by analyzing the response surface and contour plots are given as: temperature of 25 °C, acetone equivalent ratio of 4, and WHSV of 2 h^{-1}. Both the predicted and observed yields at the optimum conditions are verified as shown in Table 5. Although from the regression model and by analyzing the response surface and contour plots, a temperature lower than 25 °C, a WHSV lower than 2 h^{-1} and an acetone equivalent ratio larger than 4 would lead to even better solketal yield. However, from practical point of view, a too low temperature reduces the reaction rate, and a too small WHSV and a higher acetone equivalent ratio 4 would cause the process less economically viable (e.g., it would decrease the productivity and increase the load of distillation for solvent recovery). Moreover, the product yield at the optimum conditions was already as high as 93–94%.

3.4. Effects of impurities on the solketal yield

Assuming the presence of salt and water as impurities in the glycerol obtained from biodiesel industry, an attempt was made to check their effects on the solketal yield at the optimum conditions. Fig. 6 shows the effects of impurities on the product yield. It can be seen that the presence of water and or salt (sodium chloride) has adverse effects on the solketal yield. These effects can be explainable as the presence of water in the medium imposes a thermodynamic barrier, which limits the reaction in forward direction, and the presence of cations (Na^+) could deactivate the catalyst by cationic exchange of the protons of the acid resin catalyst, causing a decrease in the acidity of the catalyst. Similar observations have been reported for batch reactors [5,28].

From the results presented in Fig. 6, insignificant reduction in the yield was observed when replacing the ethanol solvent by methanol in the reaction, which would make the system more economical.

3.5. Catalyst life time tests

The stability of the catalyst was investigated by studying the life time of the catalyst for a longer time on stream in continuous operation. The solketal yield and glycerol conversion vs. time on stream up to 24 h from the operation under the optimum conditions (i.e., 25 °C, acetone equivalent ratio of 4, and WHSV of 2 h^{-1}) with fresh and regenerated Amberlyst 36 catalyst is shown in Fig. 7. From the figure, a decrease in the solketal yield from 94% to 89% was observed with the fresh catalyst after 24 h on stream. To recover the activity of the catalyst, it was regenerated by passing 0.5 M H_2SO_4 through the catalytic column followed by washing with methanol–water solution and drying it at 85 °C for 4 h [29]. The regenerated catalyst demonstrated almost equal initial activity as the fresh catalyst. However, the regenerated catalyst has a comparatively rapid deactivation process over the fresh catalyst: the solketal yield dropped from 95% to 85% after 24 h on stream. The catalyst deactivation was likely due to the reduction in the catalyst's acid sites (as evidenced by the results shown previously in Table 1), which might be caused by the presence of some impurities (such as water and salts) in the glycerol feed [5,28].

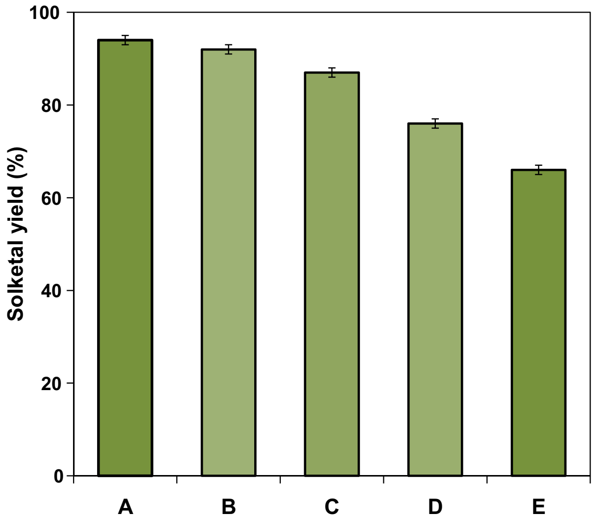

Fig. 6. Effects of impurities on the yield of solketal. (A: Ethanol as solvent; B: Methanol as solvent; C: 1 wt% NaCl in ethanol as impurity; D: 2 wt% water in ethanol as impurity; E: 1 wt% NaCl + 2 wt% water in methanol as solvent).

3.6. Economical (marginal benefit) analysis

Economical analysis is considered to be one of the key factors for the industrial production of solketal. Table 6 shows the market price for different chemicals required for the production of 1 kg of solketal. The operational cost was not considered during the cost estimation, but it is expected to be low as the mild operating conditions of our continuous flow reaction process (25 °C). Methanol and amberlyst catalyst can be recycled and reused after regeneration; hence a loss of 5 wt% and 10 wt%, respectively, is considered per operation cycle. From the table, it is clear that the production cost of solketal is approx. $1.05 /kg. The cost of solketal could be an oxygenated fuel additive or diesel combustion promoter, potential alternative to methyl tert-butyl ether (MTBE) currently used on the fuel additive market at a market price of ~$1.15 /kg. The marginal benefit is about $0.1 /kg or $100 /tonne of the solketal product. The renewable source and less environmental impact of solketal over MTBE are added advantages for solketal to replace the later as a fuel additive. Moreover, the flow reactor can be scaled up to a large scale commercial production easily, making the production of solketal more economical.

Table 5
Predicted and experimental values of the response at the optimal conditions.

Optimum conditions			Yield (%)	
Temperature (°C)	Acetone equivalent	Weight hour space velocity (h^{-1})	Experimental	Predicted
25	4	2	94.0	92.7

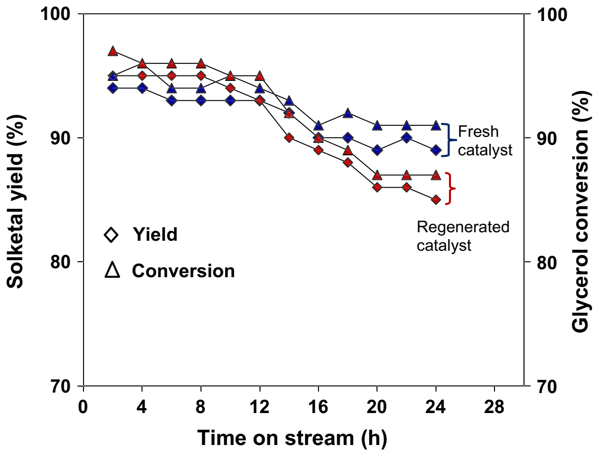

Fig. 7. Solketal yield and glycerol conversion vs. time on stream up to 24 h from the operation under the optimum conditions with fresh and regenerated Amberlyst 36 catalyst.

Table 6
Economical analysis (marginal benefit) for production of 1 kg solketal.

Chemicals	Assay (%)	Unit price ($/kg)[a]	Amount required (kg)	Cost for required amount ($)	Marginal benefit ($/kg)
Acetone	98	1	0.439	0.439	
Glycerol	98		0.697	0.348	
Amberlyst 36 wet	99	118	0.020	0.236	
Methanol	98	0.5	0.050	0.025	
Sulfuric acid	98	0.4	0.050	0.0002	
Total	–	–	–	1.05	0.10

[a] www.alibaba.com.

4. Conclusions

The process for the continuous catalytic conversion of glycerol to oxygenated fuel additive, solketal was optimized. The solid acid catalyst amberlyst – 36 Wet demonstrated an excellent catalytic performance (active, stable, and regenerable) in the flow process. A maximum solketal yield of 94 ± 2% was observed at the optimum condition (temperature: 25 °C, acetone equivalent: 4, WHSV: 2 h^{-1}). The presence of impurities like salt and water in glycerol (such as crude glycerol) reduced the yield significantly. The economical analysis demonstrated the possibility of solketal to substitute for MTBE as an oxygenated fuel additive or diesel combustion promoter.

Acknowledgements

The authors acknowledge financial support provided by Imperial Oil via University Research Award (URA) and the Discovery Grant from NSERC for Dr. Xu. We are also thankful to Professors Yasuo Ohtsuka and Guus Van Rossum from Akita University (Japan) and University of Twente (the Netherlands), respectively, for their invaluable suggestions on some aspects of this research.

References

[1] Johnson DT, Taconi KA. The glycerol glut: options for the value-added conversion of crude glycerol resulting from biodiesel production. Environ Prog 2007;26:338–48.

[2] Sun F, Chen H. Organosolv pretreatment by crude glycerol from oleochemicals chemistry for enzymatic hydrolysis of wheat straw. Bioresour Technol 2008;99:5474–9.

[3] Liu X, Jensen PR, Workman M. Bioconversion of crude glycerol feedstocks into ethanol by *Pachysolen tannophilus*. Bioresour Technol 2012;104:579–86.

[4] Clarkson JS, Walker AJ, Wood MA. Continuous reactor technology for ketal formation: an improved synthesis of solketal. Org Process Res Dev 2001;5:630–5.

[5] Vicente G, Melero JA, Morales G, Paniagua M, Martin E. Acetalization of bio-glycerol with acetone to produce solketal over sulfonic mesostructured silicas. Green Chem 2010;12:899–907.

[6] Li L, Koranyi TI, Sels BF, Pescarmmona PP. Highly efficient conversion of glycerol to solketal over heterogeneous Lewis acid catalyst. Green Chem 2012;14:1611–9.

[7] Zhou CH, Zhao H, Tong DS, Wu LM, Yu WH. Recent advances in catalytic conversion of glycerol. Catal Rev: Sci Eng 2013;55:369–453.

[8] Mota CJ, da Silva CXA, Rosenbach N, Costa J, da Silva F. Glycerine derivatives as fuel additives: the addition of glycerol/acetone ketal (solketal) in gasolines. Energy Fuels 2010;24:2733–6.

[9] Crotti C, Farnetti E, Guidolin N. Alternative intermediates for glycerol valorization: iridium-catalyzed formation of acetals and ketals. Green Chem 2010;12:2225–31.

[10] Garcia E, Laca M, Perez E, Garrido A, Peinado J. New class of acetals derived from glycerin as a biodiesel fuel component. Energy Fuels 2008;22:4274–80.

[11] Roldan L, Mallada R, Fraile JM, Mayoral JA, Menendez M. Glycerol upgrading by ketalization in a zeolite membrane reactor. Asia-Pac J Chem Eng 2009;4:279–84.

[12] Maksimov AL, Nekhaev AI, Ramazanov DN, Arinicheva YA, Dzyubenko AA, Khadzhiev SN. Preparation of high-octane oxygenate fuel components from plant-derived polyols. Pet Chem 2011;51:61–9.

[13] Ferreira P, Fonseca IM, Ramos AM, Vital J, Castanheiro JE. Valorisation of glycerol by condensation with acetone over silica-included heteropolyacids. Appl Catal B: Environ 2010;98:94–9.

[14] Yetilmezosy K, Demirel S, Vanderbei RJ. Response surface modeling of Pb (II) removal from aqueous solution by *Pistacia vera* L: Box–Behnken experimental design. J Hazard Mater 2009;171:551–62.

[15] Nanda MR, Yuan Z, Ghaziaskar HS, Poirior MA, Qin W, Xu C. Thermodynamic and kinetic studies of a catalytic process to convert glycerol into solketal as an oxygenated fuel additive. Fuel 2014;117:470–7.

[16] Nanda MR, Yuan Z, Ghaziaskar HS, Poirior MA, Qin W, Xu C. A new continuous-flow process for catalytic conversion of glycerol to oxygenated fuel additive: catalyst screening. Appl Energy 2014, in press.

[17] Xie X, Huang F, Wei X, Hu W, Ren Q, Yuan X. Modelling and optimization of pulsed green laser dicing of sapphire using response surface methodology. Optics Laser Technol 2013;45:125–31.

[18] Moradi M, Daryan JT, Mohamadalizadeh A. Response surface modelling of H_2S conversion by catalytic oxidation reaction over catalysts based on SiC nanoparticles using Box–Behnken experimental design. Fuel Process Technol 2013;109:163–71.

[19] Liu C, Sun Z, Du J. Response surface optimization of fermentation conditions for producing xylanase by *Aspergillus niger SL-05*. J Ind Microbiol Biotechnol 2008;35:703–11.

[20] Box GEP, Hunter WG, Hunter JS. Statistics for experimenters design innovation and discovery. second ed. New York: John Wiley & Sons; 2005.

[21] Sheng ZL, Li JC, Li YB. Optimization of ultrasonic-assisted extraction of phillyrin from Forssythia suspense using response surface methodology. Med Plans Res 2012;6:1633–44.

[22] Pinzi S, Lopez-Gimenez FJ, Ruiz JJ, Dorado MP. Response surface modeling to predict biodiesel yield in a multi-feedstock biodiesel production plant. Bioresour Technol 2010;101:9587–93.

[23] Montgomery DC. Design and analysis of experiments. sixth ed. New York: John Wiley & Sons; 2005.

[24] Yilmaz Y, Toledo RT. Oxygen radical absorbance grape/wine industry by-products and effect of solvent type on extraction of grape seed polyphenols. J Food Compos Anal 2006;19:41–8.

[25] Sinha K, Saha PD, Datta S. Response surface optimization and artificial neutral network modelling of microwave assisted neutral dye extraction from pomegranate rind. Ind Crop Prod 2012;37:408–14.

[26] Yin G, Dang Y. Optimization of extraction technology of the *Lycium barbarum* polysaccharides by Box–Behnken statistical design. Carbohyd Polym 2008;74:603–10.

[27] Sun Y, Liu J, Kennedy JF. Extraction optimization of antioxidant polysaccharides from the fruiting bodies of *Chroogomphis rutilus* (*Schaeff Fr*) O.K. Miller by Box–Behnken statistical design. Carbohyd Polym 2010;82:209–14.

[28] da Silva CXA, Mota CJA. The influence of impurities on the acid-catalysed reaction of glycerol with acetone. Biomass Bioenergy 2011;35:3547–51.

[29] Izci A, Hosgun HL. Kinetics of synthesis of isobutyl propionate over amberlyst-15. Turk J Chem 2007;31:493–9.